Neuropsychopharmacology (2009) 34, 374–389

www.neuropsychopharmacology.org

Reduced Dendritic Spine Density in Auditory Cortex of Subjects with Schizophrenia

Robert A Sweet*[,1,2,3], Ruth A Henteleff[1], Wei Zhang[4], Allan R Sampson[4] and David A Lewis[1,5]

[1]Department of Psychiatry, University of Pittsburgh, Pittsburgh, PA, USA; [2]Department of Neurology, University of Pittsburgh, Pittsburgh, PA, USA; [3]VISN 4 Mental Illness Research, Education and Clinical Center, VA Pittsburgh Healthcare System, Pittsburgh, PA, USA; [4]Department of Statistics, University of Pittsburgh, Pittsburgh, PA, USA; [5]Department of Neuroscience, University of Pittsburgh, Pittsburgh, PA, USA

We have previously identified reductions in mean pyramidal cell somal volume in deep layer 3 of BA 41 and 42 and reduced axon terminal density in deep layer 3 of BA 41. In other brain regions demonstrating similar deficits, reduced dendritic spine density has also been identified, leading us to hypothesize that dendritic spine density would also be reduced in BA 41 and 42. Because dendritic spines and their excitatory inputs are regulated in tandem, we further hypothesized that spine density would be correlated with axon terminal density. We used stereologic methods to quantify a marker of dendritic spines, spinophilin-immunoreactive (SP-IR) puncta, in deep layer 3 of BA 41 and 42 of 15 subjects with schizophrenia, each matched to a normal comparison subject. The effect of long-term haloperidol exposure on SP-IR puncta density was evaluated in nonhuman primates. SP-IR puncta density was significantly lower by 27.2% in deep layer 3 of BA 41 in the schizophrenia subjects, and by 22.2% in deep layer 3 of BA 42. In both BA 41 and 42, SP-IR puncta density was correlated with a marker of axon terminal density, but not with pyramidal cell somal volume. SP-IR puncta density did not differ between haloperidol-exposed and control monkeys. Lower SP-IR puncta density in deep layer 3 of BA 41 and 42 of subjects with schizophrenia may reflect concurrent reductions in excitatory afferent input. This may contribute to impairments in auditory sensory processing that are present in subjects with schizophrenia.
Neuropsychopharmacology (2009) **34,** 374–389; doi:10.1038/npp.2008.67; published online 7 May 2008

Keywords: auditory cortex; schizophrenia; synapse; dendrite; pathology

INTRODUCTION

Auditory cortex in humans is located on the superior temporal gyrus (STG), where it serves to process auditory sensory input and phonemic elements (Wessinger *et al*, 2001; Shergill *et al*, 2000; Liegeois-Chauvel *et al*, 2004). In subjects with schizophrenia, the rapid initial phases of transfer and processing of sensory information within the auditory cortex are impaired (McCarley *et al*, 1991; Javitt *et al*, 1994, 1995, 1997b, 2000; Rabinowicz *et al*, 2000). These impairments are manifest as the reduced ability to discriminate tones (Javitt *et al*, 2000; Strous *et al*, 1995; Wexler *et al*, 1998) and as deficits in recognition of prosody (Leitman *et al*, 2005).

Recently, *in vivo* studies have begun to shed light on underlying structural abnormalities within the auditory cortex of subjects with schizophrenia. For example, evaluations of studies using magnetic resonance imaging (MRI) have found that reduced gray matter volume of the STG is the most consistently reported change in cortical gray matter volume in subjects with schizophrenia (Honea *et al*, 2005; McCarley *et al*, 1999). STG gray matter volume reductions do not seem to be an artifact of illness duration or neuroleptic treatment because they are already present in subjects with schizophrenia at the time of their first psychotic episode (Hirayasu *et al*, 1998, 2000; Kasai *et al*, 2003), and in some subjects at high risk for onset of schizophrenia (Rajarethinam *et al*, 2004). Furthermore, gray matter volume reductions in STG are not found in psychotic bipolar disorder subjects (Hirayasu *et al*, 1998, 2000) and are not prominent in subjects with alcohol dependence (Mathalon *et al*, 2003; Sullivan *et al*, 1998), suggesting that these reductions reflect the disease process of schizophrenia.

In a series of post-mortem studies, we have identified a reduction in several gray matter constituents in the auditory cortex of subjects with schizophrenia (Figure 1). In deep layer 3 of the primary auditory cortex (BA 41), we observed reductions in mean pyramidal neuron somal volume (Sweet *et al*, 2004) and in the density of presumptive axon terminals (the latter identified by immunoreactivity for the small synaptic vesicle protein synaptophysin) (Sweet *et al*, 2007). In deep layer 3 of the auditory association

*Correspondence: Dr RA Sweet, Department of Psychiatry, University of Pittsburgh, Biomedical Science Tower, Rm W-1645, 3811 O'Hara Street, Pittsburgh, PA 15213-2593, USA, Tel: +1 412 383 8548, Fax: +1 412 624 9910, E-mail: sweetra@upmc.edu
Received 14 January 2008; revised 28 March 2008; accepted 31 March 2008

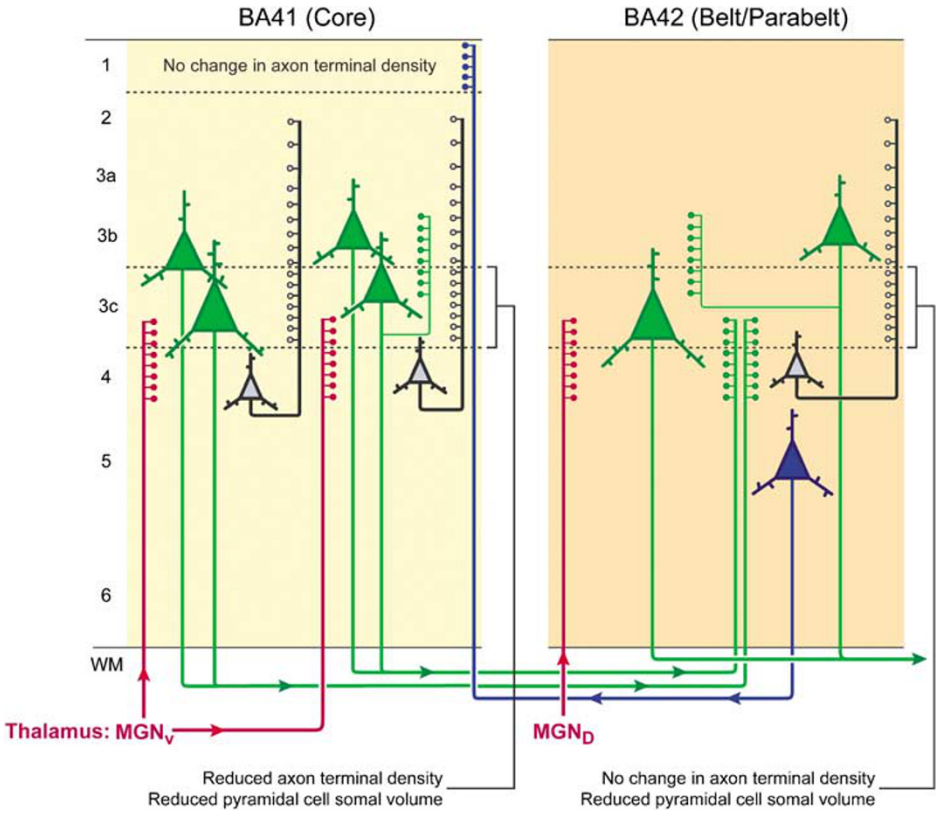

Figure 1 Schematic summary of auditory cortical circuits and alterations observed in subjects with schizophrenia. Auditory sensory processing is primarily initiated via projections (red) from the ventral subdivision of the medial geniculate nucleus of the thalamus to layers 4 and 3c of BA 41, the primary auditory (core) cortex (Pandya *et al*, 1994; Pandya and Rosene, 1993; Molinari *et al*, 1995; Hashikawa *et al*, 1995). Excitation within the core spreads through layer 3 via ascending projections from layer 4 (black) and axon collaterals from layer 3 (thin green) pyramidal cells, synapsing predominantly onto dendritic spines of layer 3 pyramidal cells (Mitani *et al*, 1985; Ojima *et al*, 1991; Wallace *et al*, 1991; Lee *et al*, 2004; Watts and Thomson, 2005). Feedforward projections from core to lateral belt (thick green) arise predominantly from layer 3 pyramidal cells (Pandya and Sanides, 1973; Jones *et al*, 1995; Galaburda and Pandya, 1983; Fitzpatrick and Imig, 1980). Feedback projections (blue) from lateral belt arise predominantly from layer 5 and terminate in layer 1 of core (Jones *et al*, 1995; Galaburda and Pandya, 1983; Pandya and Sanides, 1973; Pandya and Rosene, 1993). The same arrangement of feedforward and feedback projections exists between lateral belt and parabelt (not shown), which together consist BA 42. Layers assessed in earlier studies of subjects with schizophrenia are indicated by the dashed lines, with findings summarized as shown. MGN_V, ventral subdivision of the medial geniculate nucleus; MGN_D, dorsal subdivision of the medial geniculate nucleus.

cortex (BA 42), we also found a reduced mean pyramidal neuron somal volume in subjects with schizophrenia (Sweet *et al*, 2003), though there was not a concurrent reduction in density of axon terminals in this region (Sweet *et al*, 2007). We have interpreted this pattern of findings to represent abnormalities within the excitatory feedforward circuits of the auditory cortex in subjects with schizophrenia (Sweet *et al*, 2007). In contrast, mean pyramidal cell somal volume in layer 5 of BA 42 and axon terminal density in layer 1 of BA 41, both components of feedback pathways within auditory cortex (Jones *et al*, 1995; Galaburda and Pandya, 1983; Pandya and Sanides, 1973; Pandya and Rosene, 1993) were unaffected.

In the prefrontal cortex (PFC) of subjects with schizophrenia in which reductions in markers of axon terminal density (Glantz and Lewis, 1997; Lewis *et al*, 2001) and pyramidal cell somal volume (Rajkowska *et al*, 1998; Pierri *et al*, 2001) have been reported, reduced density of pyramidal cell dendritic spines has been identified as an additional constituent of the reduced gray matter volume. Although the relationship of dendritic spine density to pyramidal cell somal volume is not known, extensive evidence indicates that the densities of dendritic spines and excitatory axon terminals are closely related. For example, during normal developmental refinement of cortical circuitry, as dendritic spines are eliminated the presynaptic excitatory axons that terminate onto them are eliminated in tandem (Hensch, 2005). Similarly, a number of studies indicate that experimentally induced reductions in excitatory afferent input can result in reduced dendritic spine density (Cheng *et al*, 1997; Segal *et al*, 2003; McKinney *et al*, 1999; Ingham *et al*, 1993). However, the relationship between axon terminal density and dendritic spine density in subjects with schizophrenia has not been evaluated.

We therefore examined a marker of dendritic spine density in the same cohort of subjects in whom we had previously characterized pyramidal cell somal volume and axon terminal density in deep layer 3 of BA 41 and 42. We hypothesized that dendritic spine density would be reduced in these regions in subjects with schizophrenia, and correlated with axon terminal density. We also examined the relationship of dendritic spine density to mean pyramidal cell somal volume.

METHODS

Subjects

We studied the same subjects diagnosed with schizophrenia or schizoaffective disorder who had been included in our earlier studies of pyramidal cell somal volume (Sweet *et al*, 2003, 2004) and axon terminal density (Sweet *et al*, 2007). Each subject had been previously matched to one normal comparison subject for gender, and as closely as possible for age and post-mortem interval (PMI, Table 1). All brain specimens were obtained during autopsies conducted at the Allegheny County Medical Examiner's Office, after receiving consent from the next of kin using a mechanism approved by the University of Pittsburgh Institutional Review Board and Committee for Oversight of Research Involving the Dead. An independent committee of experienced clinicians made consensus DSM-III-R (American Psychiatric Association, 1987) diagnoses for each subject, using all available information from clinical records and from structured interviews conducted with surviving relatives of the deceased. Individual subjects had been primarily treated with conventional antipsychotic medications. At time of death, eight (53%) of subjects were using only conventional antipsychotic medications, four (27%) were using only atypical antipsychotic medications, one (7%) was using both, and two (13%) were using neither. The corresponding values for lifetime use of conventional and atypical antipsychotic medications were 9 (60%), 1 (7%), 4 (27%), and 1 (7%).

Tissue Preparation

The left hemisphere of each brain was blocked coronally at 1.0–2.0 cm intervals, immersed in cold 4% paraformaldehyde in phosphate buffer for 48 h, washed in a series of graded sucrose solutions, and stored in an antifreeze solution (30% glycerol and 30% ethylene glycol in phosphate-buffered saline (24 mM, pH 7.2–7.4)) at -30°C. Tissue blocks caudal to the level of the mammillary bodies and rostral to the crux of the fornix (Shenton *et al*, 1992), and matched on rostral–caudal level within subject pairs, had coronal cryostat sections (40 μm) cut throughout (Sweet *et al*, 2003, 2004). Sections were then stored in antifreeze solution at -30°C until used in this study. Total duration of tissue storage ($\pm$ SD) did not differ between the normal comparison subjects and the subjects with schizophrenia (144.1 ± 27.5 and 144.5 ± 23.9 months, respectively, $t_{28} = -0.04$, $p = 0.96$).

In our earlier studies, every 10th section (with a random start) had been processed and stained for Nissl substance, with BA 41 and 42 identified using cytoarchitectonic criteria (Sweet *et al*, 2004). Three sections separated by a minimum of 1200 μm, in which the BA 41 and 42 were cut in an orientation perpendicular to the pial surface, had been studied (Sweet *et al*, 2003, 2004). Sections adjacent to these previously studied sections were processed for spinophilin immunoreactivity. Due to limited availability of the anti-spinophilin antibody, for five pairs only two sections per subject could be processed.

Spinophilin is a protein phosphatase 1-binding protein localized predominantly in dendritic spines in primate cortex (Allen *et al*, 1997; Muly *et al*, 2004), where it labels 93–94% of spines (Tang *et al*, 2004; Hao *et al*, 2003), with some minor labeling of dendrites and glia (Muly *et al*, 2004). In the current project we utilized an affinity-purified polyclonal rabbit antibody raised against a synthetic peptide corresponding to amino acids 286–390 from rat spinophilin (Chemicon, Temecula, CA, AB5669). In primary neuronal culture this antibody selectively labels dendritic spines (Amateau and McCarthy, 2002). In immunocytochemical studies of human cortex, labeling was selective for gray matter (Figure 2e), where crisp punctate labeling of neuropil in a distribution consistent with labeling restricted to dendritic spines was seen (Figure 3b).

Free-floating tissue sections from both members of a subject pair were processed together within immunocytochemistry runs. Sections were incubated with a 1 : 2000 dilution of anti-spinophilin antibody for 96 h at 4°C, followed by incubation for 24 h at 4°C with a 1 : 200 dilution of biotinylated donkey anti-rabbit secondary antibody (711-066-152; Jackson, West Grove, PA), and for 24 h at 4°C with Cy3-streptavidin conjugate (016-160-084; Jackson) at a dilution of 1 : 500. After drying for 1 h, sections were rehydrated for 10 min in distilled water, an approach that reduces *z*-axis tissue shrinkage and therefore increases counting accuracy by enhancing the ability to resolve objects in the *z* axis (Konopaske *et al*, 2008). Sections were coverslipped with Vectashield hard set (H-1400; Vector, Burlingame, CA).

Antipsychotic-Exposed Monkeys

To assess the possible influence of antipsychotic medications, we studied four male macaque monkeys (*Macaca fascicularis*) administered the antipsychotic, haloperidol decanoate, and four control animals matched for sex, age, and weight (Akil *et al*, 1999). The mean (SD) dose of haloperidol decanoate was 16.0 (2.1) mg per kg, administered by injection every 4 weeks, yielding trough serum haloperidol concentrations of 4.3 (1.1) ng per ml. Similar concentrations have been associated with a therapeutic response in humans (Volavka *et al*, 1992), and resulted in extrapyramidal symptoms that were effectively controlled with maintenance administration of benztropine mesylate in all treated animals. After 9–12 months of haloperidol administration, animals were euthanized by pentobarbital overdose. Brains were removed and, after a 45-min PMI, coronal tissue blocks from the left hemisphere were fixed by immersion in 4% paraformaldehyde. All procedures were approved by the University of Pittsburgh's Institutional Animal Care and Use Committee.

The auditory parabelt cortex (corresponding to that portion of human BA 42 located on the planum temporale and examined in this study) was identified using cytoarchitectonic criteria (Sweet *et al*, 2005), and three sections per animal were selected (Sweet *et al*, 2005). Free-floating tissue sections from each pair were processed together within immunocytochemistry runs. Because subsequent lots of the anti-spinophilin antibody used in the human subjects showed loss of specific labeling in immunocytochemistry, we utilized a different affinity-purified polyclonal rabbit antibody (N5037; Sigma, St Louis, MO). This antibody was raised against a synthetic peptide corresponding to amino

Table 1 Subject Characteristics

	Normal comparison subjects							Schizophrenic subjects							
Pair	**Case**	**Sex/ Age**	**Race**	**Hand**	**PMI**	**Storage time**	**Cause of death**	**Case**	**Diagnosis**	**Sex/ Age**	**Race**	**Hand**	**PMI**	**Storage time**	**Cause of death**
1	250	F/47	W	R	5.3	178.22	ASCVD	398	Schizoaffective disorder	F/41	W	NA	10.3	154.29	Pulmonary embolism
2	620	M/64	W	R	17.3	103.45	Accidental drowning	566	Chronic undifferentiated schizophrenia[a]	M/63	W	R	18.3	112.89	ASCVD
3	681	M/51	W	R	11.6	98.54	Hypertrophic cardiomyopathy	234	Chronic paranoid schizophrenia[b]	M/51	W	R	12.8	181.20	Cardiomyopathy
4	643	M/50	W	R	24.0	100.67	ASCVD	581	Chronic paranoid schizophrenia[c,d]	M/46	W	M	28.1	110.54	Accidental combined drug overdose
5	634	M/52	W	L	16.2	101.88	ASCVD	625	Chronic disorganized schizophrenia[e]	M/49	B	R	23.5	103.08	ASCVD
6	474	F/49	B	NA	13.4	131.13	Hypertensive cardiovascular disease	656	Schizoaffective disorder[c]	F/47	B	R	20.1	99.23	Suicide by gunshot
7	396	M/41	W	L	17.5	154.62	ASCVD	408	Chronic paranoid schizophrenia	M/46	W	R	19.8	152.49	ASCVD
8	449	F/47	W	L	4.3	142.69	Accidental carbon monoxide poisoning	517	Chronic disorganized schizophrenia[c]	F/48	W	R	3.7	128.09	Intracerebral hemorrhage
9	451	M/48	W	L	12.0	142.51	ASCVD	317	Chronic undifferentiated schizophrenia	M/48	W	NA	8.3	173.98	Bronchopneumonia
10	178	M/48	W	R	7.8	194.43	ASCVD	377	Chronic undifferentiated schizophrenia[c]	M/52	W	R	10.0	165.17	Gastrointestinal bleeding
11	412	M/42	W	R	14.2	157.00	Aortic stenosis	466	Chronic undifferentiated schizophrenia	M/48	B	NA	19.0	140.47	ASCVD
12	285	F/27	W	R	16.5	179.03	Trauma	587	Chronic undifferentiated schizophrenia[a]	F/38	B	R	17.8	117.40	Myocardial hypertrophy
13	575	F/55	B	R	11.3	119.24	ASCVD	597	Schizoaffective disorder	F/46	W	L	10.1	115.83	Pneumonia
14	592	M/41	B	R	22.1	116.53	ASCVD	450	Chronic undifferentiated schizophrenia[b,f,g]	M/48	B	L	22.0	142.82	Suicide by jumping
15	452	F/40	W	R	14.3	142.33	ASCVD	341	Chronic undifferentiated schizophrenia[e]	F/47	W	L	14.5	171.27	Suicide by drug overdose

ASCVD, arteriosclerotic cardiovascular disease; COPD, chronic obstructive pulmonary disease; NA, not available; M, mixed; PMI, post-mortem interval (in hours); NA, not available; B, black; W, white.
PMI was significantly longer in subjects with schizophrenia ($p = 0.03$); storage time is in months.
Hand indicates handedness.
[a]Alcohol abuse, in remission at time of death.
[b]Schizophrenic subjects off medications at time of death.
[c]Alcohol dependence, current at time of death.
[d]Other substance abuse, current at time of death.
[e]Alcohol abuse, current at time of death.
[f]Alcohol dependence, in remission at time of death.
[g]Other substance dependence, in remission at time of death.

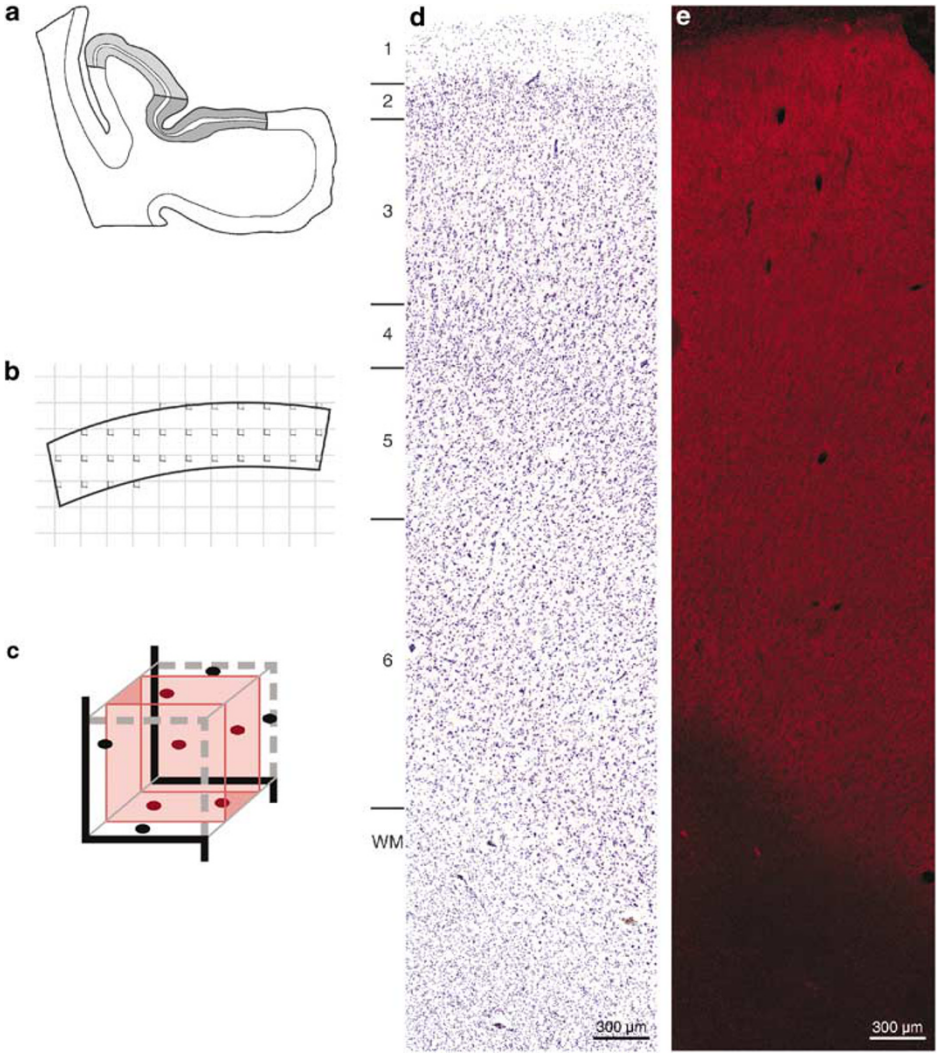

Figure 2 Summary of the method used to quantify spinophilin-immunoreactive (SP-IR) puncta. (a) Schematic of a coronal section through Heschl's gyrus and the planum temporale showing the location of BA 41 (light gray) and 42 (dark gray). Contours (clear zones) for quantification in deep layer 3 are shown. (b) Representative sampling grid systematic randomly overlaid on a contour. (c) An enlarged view of an optical disector from the sampling grid shown in (b). The solid and dashed lines show the boundaries of the counting frame, represented at the top and bottom of the section's *z*-axis thickness. The zone of uniform SP-IR puncta density sampled in the middle 50% of the *z*-axis thickness (see also Figure 5) is shown by the red band. (d) Photomicrograph of BA 42 from a normal comparison subject processed for Nissl substance. The distinctive cytoarchitectonic features of BA 42 are evident: broad, densely granular layers 2 and 4; large pyramidal neurons in deep layer 3; and a relatively hypocellular layer 5. (e) Confocal micrograph (XY Montage) of an adjacent section processed for spinophilin immunoreactivity. Intense labeling is evident throughout all cortical layers, with little to no label in the white matter.

acids 800–817 from rat spinophilin. After stripping western blots of monkey and human cortical protein extracts that had been probed with the anti-spinophilin antibody used in our human subjects, this antibody recognizes the identical band (data not shown). The selectivity of this antibody for dendritic spines was confirmed in primary neuronal culture derived from embryonic rat hippocampus (provided by Dr KN Fish, prepared as previously described (Aridor *et al*, 2004) using labeling by phalloidin to identify spines (Capani *et al*, 2001); Figure 3a). Immunocytochemical studies of monkey cortex using this antibody (Figure 3c) reveals predominantly punctate labeling of neuropil in a distribution consistent with labeling of dendritic spines. After a 30 min preincubation in 1% sodium borohydride (S-9125; Sigma), sections were incubated with a 1 : 2000 dilution of anti-spinophilin antibody for 96 h at 4°C, followed by incubation for 24 h at 4°C with a 1 : 200 dilution of biotinylated donkey anti-rabbit secondary antibody (711-066-152; Jackson), and for 24 h at 4°C with Cy3-streptavidin conjugate (016-160-084; Jackson) at a dilution of 1 : 500. All incubations were done in buffer including 0.3% Triton X (Sigma X-100), 5% normal human serum (009-000-121; Jackson), 5% normal donkey serum (017-000-121; Jackson), 1% BSA (A2153; Sigma), 0.1% D-lysine monohydrochloride (Sigma, L5876), and 0.1% glycine (G7403; Sigma). Sections were coverslipped with Vectashield hard set (H-1400; Vector).

Quantification of SP-IR Puncta

One investigator (RAH) performed quantification in human and monkey, without knowledge of diagnosis or group

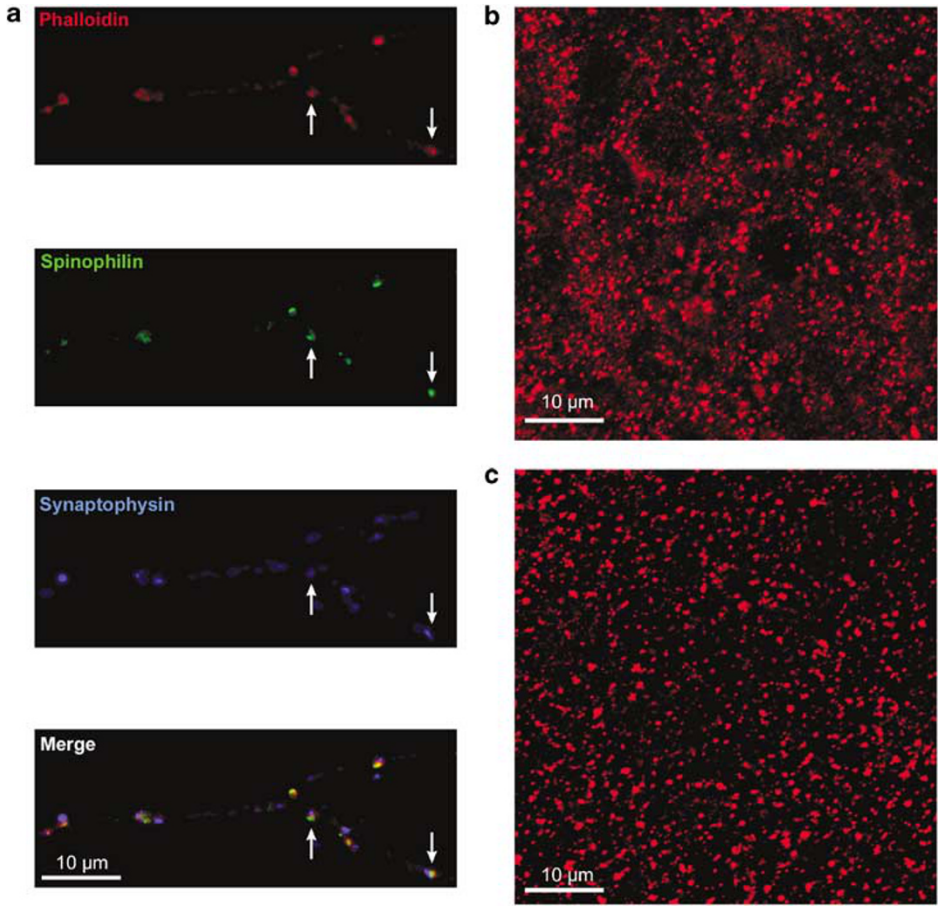

Figure 3 Spinophilin-immunoreactive (SP-IR) puncta in human and antipsychotic-exposed monkey. (a) Labeling of dendritic spines by the anti-spinophilin antibody utilized for studies of monkey tissue in mature primary neuronal culture. A dendrite with spines labeled with phalloidin can be clearly seen to colocalize spinophilin. Axon terminals labeled by antibody to synaptophysin appose some of these spines (arrows). (b) Confocal projection micrograph of spinophilin immunoreactivity in human cortex showing labeled puncta from deep layer 3 of Figure 2e at higher magnification. (c) SP-IR puncta, labeled using the same antibody as in (a), shown in deep layer 3 of monkey auditory cortex.

assignment. Presumptive dendritic spines were defined as spinophilin-immunoreactive (SP-IR) punctate structures with intense labeling, and were readily distinguished from background fluorescence (Figure 3b and c; Supplementary Movie 1). Earlier studies have demonstrated that stereologic quantification of SP-IR puncta counts were sensitive to detection of spine density differences induced by experimental manipulations in nonhuman primates (Tang *et al*, 2004; Hao *et al*, 2003). Labeled puncta were quantified using a Zeiss Axioplan microscope with motorized *z*-axis controller and specimen stage (Ludl Electronic Products, Hawthorne, NY), MT12 microcator and ND281 readout (Heidenhain, Germany), CCD camcorder (Optronics DEI-750T, Goleta, CA), and a computer with Stereo Investigator software, Version 5.05.4 (MicroBrightField Inc., Colchester, VT). SP-IR puncta were visualized using a mercury short-arc lamp (HBO103W/2; Osram, Munich, Germany) and a Zeiss Filter Set 15, with a band-pass 546 ± 6 nm excitation filter and a long-pass 690 nm emission filter (Carl Zeiss Inc., Thornwood, NY). The borders of layers 2/3 and 3/4 in BA 41 and 42 were identified in the Nissl-stained sections to determine the thickness of layer 3 (Figure 2d). To evaluate a region of interest comparable to our earlier studies (Sweet *et al*, 2003, 2004), contours outlining the deepest 1/3 of layer 3 were drawn. Contours were aligned with the adjacent spinophilin-labeled sections using pial surface fiduciaries (Sweet *et al*, 2007). Counts of SP-IR puncta were obtained using a 1.4 numerical aperture, $\times 100$, oil immersion objective visualized on a computer monitor at a final magnification of $\times 4450$.

Sampling of SP-IR Puncta

We conducted initial studies to assess the susceptibility of the immunofluorescent labeling to bleaching and quenching effects during quantification. At any given sampling site puncta counts did not diminish unless there was continuous excitation lasting longer than 6 min, greater than the approximately 1 min required to quantify a single site (Figure 4a). Moreover, there was no evidence of progressive diminution of counts within a single section as a function of the total sampling duration, ie counts at the last sampled sites were not systematically lower than at the initially sampled sites (Figure 4b).

Additional pilot studies assessed antibody penetration and were used to develop appropriate sampling criteria. One slide from each of three subjects was sampled throughout the *z* axis in area BA 41 deep layer 3 or BA 42

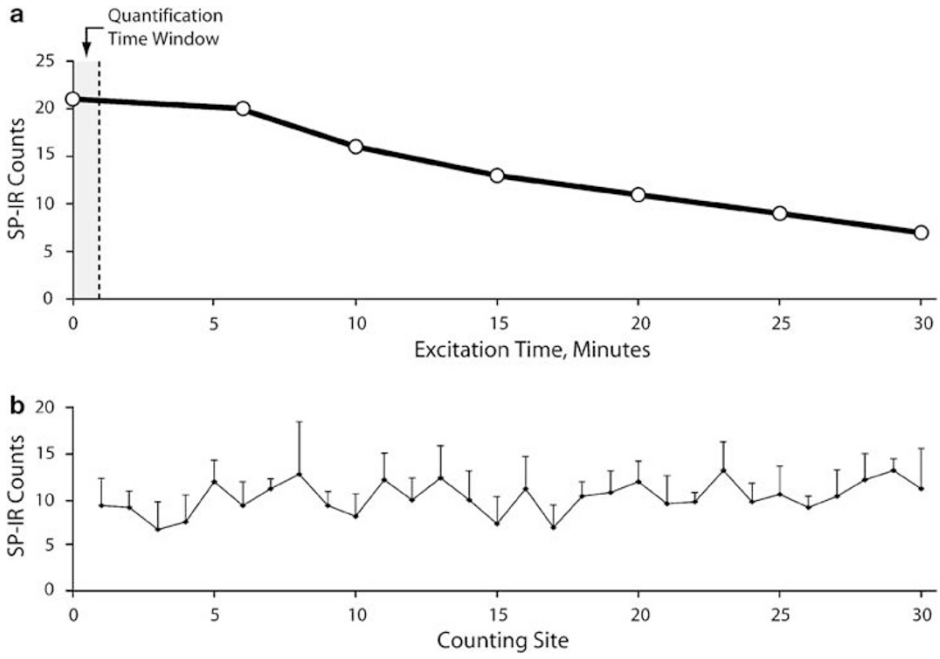

Figure 4 Absence of photobleaching and quenching effects on quantification of spinophilin-immunoreactive (SP-IR) puncta. (a) Counts of SP-IR puncta at a single site during continuous fluorescent excitation. Counts were obtained using a × 100, 1.4NA oil immersion objective. All puncta within a 3.5 × 3.5 μm counting frame throughout the entire section thickness were counted at approximately 5 min intervals. (b) Mean (SEM) counts of SP-IR puncta, similarly obtained at each of multiple sites within sections. Each section was sampled during a single session with continuous fluorescent excitation.

deep layer 3, using an optical disector approach (Gundersen, 1986). SP-IR counts were plotted as a function of tissue thickness in 2.0 μm depth intervals. Antibody penetration was uniform throughout the *z*-axis depth of the tissue, though due to presumed cutting artifacts at the tissue surfaces (Dorph-Petersen *et al*, 2001), SP-IR counts were reduced in the tissue surface. On the basis of pilot data, we used a disector height set at 50% of the measured tissue thickness at each site, with guard zones of 25% of the measured tissue thickness at each site. This approach resulted in sampling from a region of consistent antibody penetration in both regions for all subjects (Figure 5).

Since the area of the delineated contours varied between subjects, to target sampling 200 SP-IR puncta per region per case (Gundersen *et al*, 1999), we adjusted the proportion of area sampled (area sampling fraction). The area sampling fraction was maintained constant within subjects, ie no tissue section was sampled more intensively than any other section for each subject. The resultant sampling grid for each subject was randomly superimposed over the contour. SP-IR puncta were counted at each site with the *z*-axis depth of each terminal automatically recorded. A unique associated point for each counting frame was used to estimate the number of counting frames falling within each contour. Section thickness was measured at each counting site. This approach resulted in a final mean (SD) puncta counted per subject in BA 41 of 466 (203), ranging from 123 to 1064 per subject. In BA 42 the corresponding values were 517 (217) with a range from 127 to 932. Final mean section thicknesses (SD) in control and schizophrenia subjects did not differ in BA 41, 17.7 (2.72) and 17.85 μm (3.6), $t_{28} = -0.03$, $p = 0.98$, and in BA 42 19.3 (2.5) and 18.6 μm (3.0), $t_{28} = 0.70$, $p = 0.49$.

SP-IR puncta density values were calculated as follows:

$$\text{density} = \left(\frac{\text{Q}}{\text{CF} * 12.25 * 20}\right).$$

Q, the number of SP-IR puncta counted within a section; CF, estimated number of counting frames per section; 12.25, area of a counting frame in microns; 20, disector height in microns of cut tissue thickness (by definition 50% of the cryostat block advance of 40 μm).

Coefficient of error (CE) calculations for puncta densities were as described in Braendgaard *et al* (1990). CEs for BA 41 deep layer 3 were 0.17 and 0.16 in comparison subjects and subjects with schizophrenia, respectively. The corresponding CE's in BA 42 deep layer 3 were 0.17 and 0.14. Providing evidence of the limited contribution of measurement error to the determination of SP-IR puncta densities, determination of SP-IR puncta density was repeated in five contours from three subjects, yielding an intraclass correlation coefficient of 0.90.

Statistical Methods

For each subject, puncta densities were calculated for each section and region of interest. Preliminary multivariate analyses of covariance (MANCOVA) demonstrated no evidence that slide order (rostral to caudal) or immunocytochemistry run had differential effects on diagnosis for SP-IR puncta densities. A two-sample *t*-test (see below) demonstrated no evidence that subject handedness had a differential effect on diagnosis for SR-IR puncta densities. Thus, the subsequent analyses of SP-IR puncta densities did not take these factors into account.

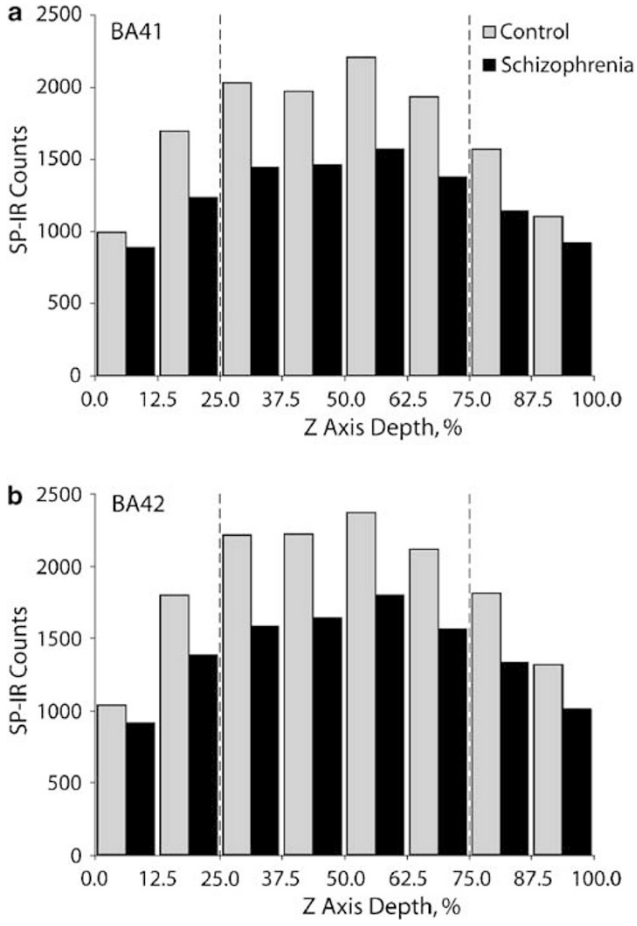

Figure 5 Panels (a) (BA41) and (b) (BA42) show the frequency distribution of spinophilin-immunoreactive puncta within the cut section thickness of 40-μm (*z* axis) for all subjects. Spinophilin-immunoreactive puncta were quantified at each site and the *z* axis depth of each puncta recorded. Total puncta counted in bins representing 12.5% of the *z* axis depth at each site are shown (tissue surface, 0%; surface of the slide, 100%). The vertical reference lines indicate the *z* axis position of the top and bottom of the disector, respectively, i.e., spinophilin-immunoreactive puncta density was calculated based on counts obtained from the zone between these lines. It can be clearly seen that puncta counts were uniform throughout this zone, indicating consistent immunolabeling and the absence of cutting artifacts.

Analyses of each region of interest separately used a MANCOVA with interclass covariate structure and treated observations from the three sections per subject as repeated measures. Two MANCOVA models were utilized: a primary model with diagnosis, pair as a blocking factor and, because subjects were not paired on tissue storage time, tissue storage time as a covariate; and a secondary model with diagnosis, gender, age, PMI, and tissue storage time entered as covariates with subject pairings ignored. Analyses were implemented in SAS PROC Mixed (Littell *et al*, 1996) where the degrees of freedom method was Kenward–Roger.

Two-sample *t*-tests using the average of each subject's density values were used to examine the effects of antipsychotic use, alcohol dependence, suicide, and schizoaffective disorder. The percent change of the subject with schizophrenia relative to the normal comparison subject within each pair was computed as the dependent variable. The effects of duration of illness and age of onset were assessed using linear regression models (excluding pair (11) for which age of onset and duration values were missing). To examine further SP-IR puncta densities, the primary (MANCOVA) model described in the previous paragraph was implemented in each region only for subjects who did not have a history of death by suicide.

Pearson's correlation coefficients were calculated in BA 41 and 42 to examine the relationship among mean pyramidal cell somal volume, axon terminal density, and SP-IR puncta density based on all subjects' data.

For antipsychotic-exposed monkeys, for each animal, the average SP-IR puncta densities were calculated. A paired *t*-test (with d.f. = 3) was used to compare the average SP-IR puncta densities between antipsychotic-exposed and control animals. Due to the similarity of storage time across the pair, storage time was not used as a covariate.

All statistical tests were conducted at the 0.05 significance level.

RESULTS

BA 41 Deep Layer 3

The density of SP-IR puncta in deep layer 3 of BA 41 was significantly decreased in subjects with schizophrenia in both the primary ($F(1,13.3) = 10.16$, $p = 0.007$) and secondary ($F(1,23.3) = 6.10$, $p = 0.02$) statistical models. The latter did not reveal an association of puncta density with age, gender, PMI, or storage time. Estimated mean (95% CI) SP-IR puncta densities derived from the primary model were 0.0276 (0.0240, 0.0313) and 0.201 puncta per μm^3 (0.0165, 0.0237) in normal comparison subjects and subjects with schizophrenia, respectively, a 27.2% reduction in the subjects with schizophrenia (Figure 6).

BA 42 Deep Layer 3

The density of SP-IR puncta in deep layer 3 of BA 42 was significantly decreased in subjects with schizophrenia in the primary model ($F(1,12.6) = 10.02$, $p = 0.008$) and nearly so ($F(1,23.5) = 4.12$, $p = 0.054$) in the secondary statistical model. The latter also revealed an association of decreased puncta density with increased PMI ($F(1,25) = 5.12$, $p = 0.03$). Estimated mean (95% CI) SP-IR puncta densities derived from the primary model were 0.0302 (0.0269, 0.0334) and 0.0235 puncta per μm^3 (0.0203, 0.0267) in normal comparison subjects and subjects with schizophrenia, respectively, a 22.2% reduction in the subjects with schizophrenia.

Potential Clinical Confounds

The density of SP-IR puncta did not significantly differ when contrasting subject pairs in which the schizophrenia subject (1) was on *vs* off antipsychotic treatment at the time of death (BA 41 $t(13) = -0.072$, $p = 0.48$, BA 42 $t(13) = -0.066$, $p = 0.52$); (2) did or did not have comorbid alcohol dependence (BA 41 $t(13) = 0.452$, $p = 0.66$, BA 42 $t(13) = 1.02$, $p = 0.32$); or (3) received a diagnosis of schizophrenia *vs* a diagnosis of schizoaffective disorder (BA 41 $t(13) = -0.23$, $p = 0.82$, BA 42 $t(13) = 0.69$, $p = 0.50$). Age of onset of schizophrenia (BA 41 $r = -0.09$, $p = 0.74$, BA 42 $r = 0.02$,

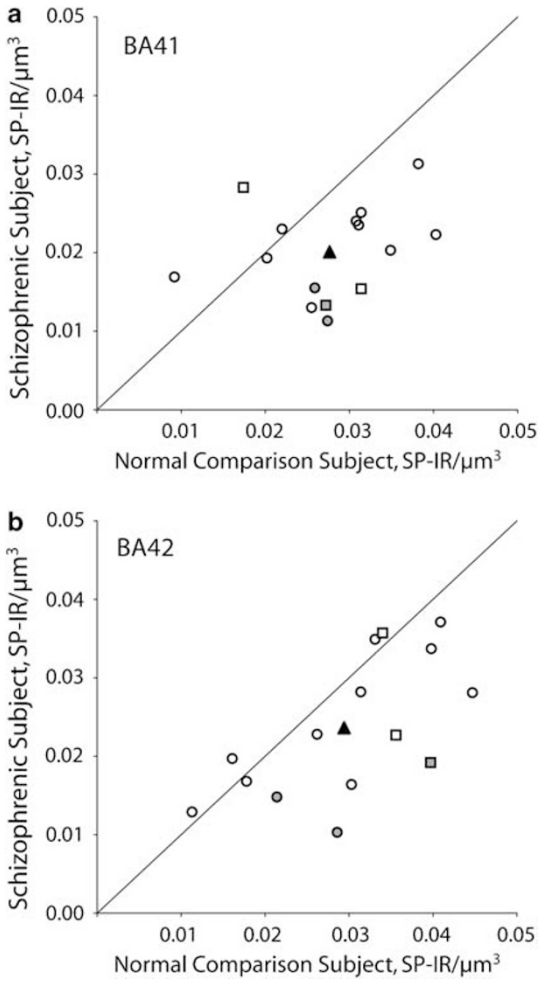

Figure 6 Spinophilin-immunoreactive (SP-IR) puncta densities in deep layer 3 of BA 41 (a) and BA 42 (b). In all panels, densities are shown as number of SP-IR puncta/μm^3. Each circle represents a pair with the comparison subject's mean puncta density value represented on the *x* axis and the schizophrenia subject's value on the *y* axis. Squares represent pairs with schizoaffective subjects (pairs 1, 6, and 13). Shaded circles and squares indicate pairs in which the subject with schizophrenia/schizoaffective disorder died due to suicide. Filled triangles denote group means. Markers below the diagonal reference line indicate pairs for which the schizophrenia or schizoaffective subject had a lower mean puncta density than the matched comparison subject.

$p = 0.95$) and duration of illness (BA 41 $r = -0.05$, $p = 0.87$, BA 42 $r = -0.06$, $p = 0.82$) were not significantly correlated with the percent change (relative to the matched control subject) in puncta density in either region. There was, however, a significant association between a history of death by suicide and percent reduction in SP-IR puncta density in both BA 41 and 42 ($t(13) = 2.92$, $p = 0.01$ and $t(3.8) = 3.33$, $p = 0.03$, respectively). In BA 41 the mean (SD) percent reduction in SP-IR puncta density for subject pairs in which the subject with schizophrenia had died by suicide was 49.9% (9.4), whereas for subject pairs in which the subject with schizophrenia had died in other manners it was 10.4% (42.9). The corresponding values in BA 42 were 48.5 (16.7) and 10.5% (21.1). To assess whether the observed reductions in SP-IR density were confined to subjects with death by suicide, we reanalyzed our primary model after excluding these three subject pairs. Evidence of lower SP-IR density was persistent for the remaining 12 pairs in both BA 41 and 42 ($F(1,10.7) = 4.54$, $p = 0.06$ and $F(1,11.1) = 4.72$, $p = 0.05$).

Effects of Pyramidal Cell Somal Volume and Axon Terminal Density Reductions

We examined whether SP-IR puncta density was correlated with our earlier observations of axon terminal density and pyramidal cell somal volume in the same regions and subjects (Figure 7). Significant correlations of SP-IR and axon terminal densities were seen in both BA 41 and 42. In contrast, SP-IR density was not correlated with pyramidal cell somal volume in either region.

Antipsychotic-Exposed Monkeys

Mean (SD) SP-IR puncta densities were 0.0375 (0.006) and 0.0383 puncta per μm^3 (0.012) in control animals and in antipsychotic-exposed animals, respectively. The density of SP-IR puncta in deep layer 3 of auditory parabelt did not significantly differ between antipsychotic-exposed and control animals (mean difference (95% CI) −0.0008 (−0.0265, 0.0250), $t(3) = -0.09$, $p = 0.93$).

DISCUSSION

We have previously identified a number of abnormalities within the auditory cortex of subjects with schizophrenia, including reduced mean somal volumes of pyramidal cells in deep layer 3 of BA 41 and 42 (Sweet *et al*, 2003, 2004) and reduced density of a marker of axon terminals, synaptophysin-immunoreactive puncta, in deep layer 3 of BA 41 in the same subjects. Complementing these earlier findings, we now report that density of a marker of dendritic spines, SP-IR puncta, is also reduced in deep layer 3 of BA 41 and 42. Reduced dendritic spine density was not associated with a history of antipsychotic treatment at time of death, or with antipsychotic exposure in a nonhuman primate model. The magnitude of dendritic spine density reduction was greater in individuals with a history of death by suicide. Within subjects, dendritic spine density was correlated with axon terminal density, but not with mean pyramidal cell somal volume.

Interpretive Issues

An important consideration is whether the reduction in SP-IR puncta density in our subjects with schizophrenia resulted from a reduced density of dendritic spines, or a reduced detectability of spinophilin protein, as mice lacking spinophilin demonstrate increased or normal spine density (Feng *et al*, 2000). We used a stereologic approach to count individual SP-IR puncta. In nonhuman primate a similar approach detected estrogen-induced increases in hippocampal spine density (Hao *et al*, 2003), findings that parallel the estrogen-induced changes in spine density measured using Golgi preparations or ultrastructural quantification via electron microscopy (EM, Leranth *et al*, 2002). Similarly, in individuals with Alzheimer's disease, stereologic assessment of SP-IR puncta number has been correlated with the extent of neurodegenerative lesions and with the degree of

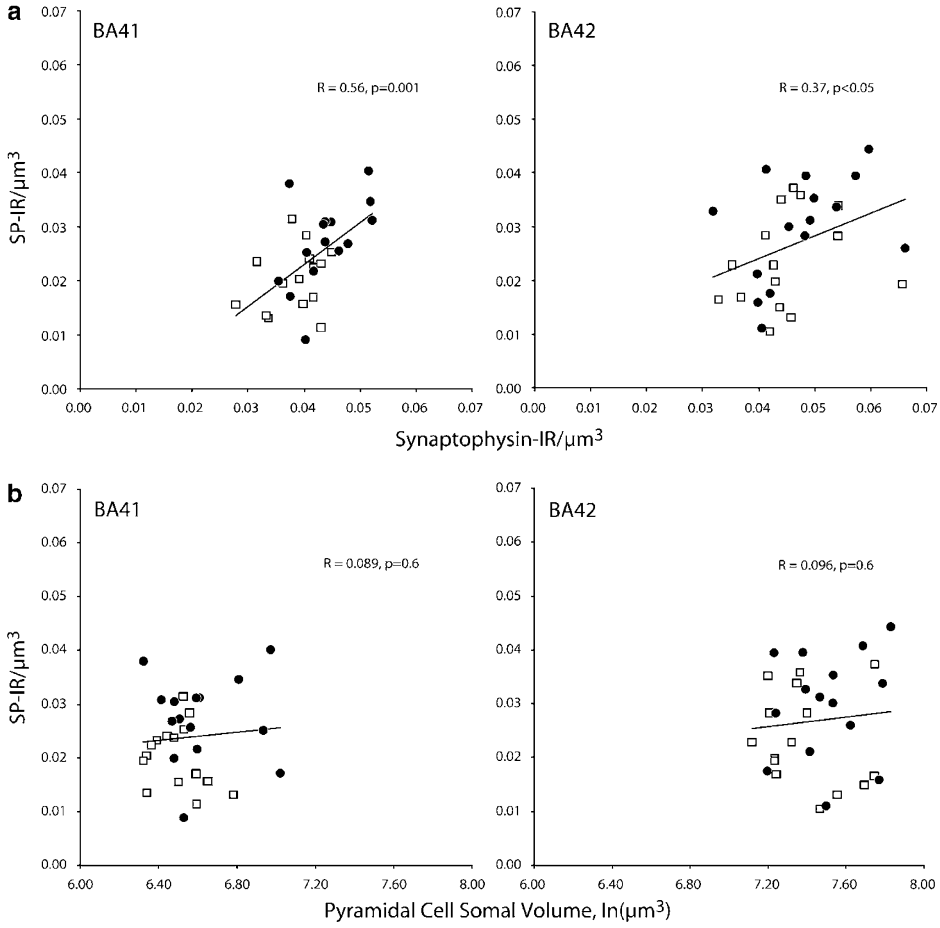

Figure 7 Correlations of spinophilin-immunoreactive puncta densities in deep layer 3 of BA41 and BA42 with axon terminal density (a) and pyramidal cell somal volume (b) in the same locations. Filled circles represent comparison subjects, squares subjects with schizophrenia.

cognitive impairment (Akram *et al*, 2007), both of which reflect degree of synapse loss (Scheff and Price, 2003). Moreover, there is little evidence to suggest that spinophilin detectability is reduced in subjects with schizophrenia. In the one prior study to examine spinophilin protein expression in subjects with schizophrenia, no change was found using slot blots of dorsolateral PFC (Koh *et al*, 2003). Examinations of spinophilin mRNA expression have yielded mixed results. Elevations in spinophilin mRNA across all cortical layers in PFC were reported in one study (Baracskay *et al*, 2006), whereas no change expression has been reported in anterior cingulate cortex in the same subjects (Baracskay *et al*, 2006) and in thalamus from the same brain tissue collection (Clinton *et al*, 2005). A study of PFC in a different cohort found no change in spinophilin mRNA expression in subjects with schizophrenia (Weickert *et al*, 2004). One report found reduced spinophilin mRNA expression in hippocampus of subjects with schizophrenia (Law *et al*, 2004b). Thus, the reduced density of SP-IR puncta we observed is likely to reflect a reduction in dendritic spine density rather than a reduced expression of spinophilin.

Whether the reduction in dendritic spine density results from a reduction in number of dendritic spines, or from expansion of the surrounding tissue volume, also needs to be considered. *In vivo* studies indicate that gray matter volume is reduced in the STG of subjects with schizophrenia (reviewed in McCarley *et al*, 1999; see also Sanfilpo *et al*, 2000; Sigmundsson *et al*, 2001; Mathalon *et al*, 2001; Goldstein *et al*, 1999). The *in vivo* evidence includes reduced volume of Heschl's gyrus that contains BA 41, although the volume reduction in Heschl's gyrus may be smaller than that in the adjacent auditory association cortex containing BA 42 (Barta *et al*, 1997; Kwon *et al*, 1999; Hirayasu *et al*, 2000). Similarly, there is evidence in post-mortem studies of reduced gray matter volume of STG in subjects with schizophrenia (Falkai *et al*, 1995; Vogeley *et al*, 1998; Highley *et al*, 1999); however, none of these studies examined gray matter volumes of specific cytoarchitectonic or chemoarchitectonic regions within STG. In contrast, we recently reported that total volume of the auditory parabelt (analogous in location to the region of BA 42 examined in the present study), and of layer 3 within the parabelt, was reduced in subjects with schizophrenia (Marcsisin *et al*, 2007). In BA 41, total and layer 3 volumes were not significantly smaller in subjects with schizophrenia than in control subjects. Because the effects of reductions in density and in regional volume on spine number are additive, the most likely interpretation of the reduction in density of SP-IR puncta in our subjects with schizophrenia is that it reflects reduced numbers of dendritic spines in these regions.

Finally, it needs to be considered whether the observed reduction in spine numbers in the neuropil reflects fewer spines per unit length of dendrite or normal spine number per dendritic length, but in the presence of a reduction in total dendritic length. Though this question cannot be resolved within the current study, earlier studies have used Golgi preparations to examine both these dendritic parameters in subjects with schizophrenia. These studies have found lower spine density per dendritic length in subjects with schizophrenia on pyramidal neurons located in deep layer 3 of PFC (Glantz and Lewis, 2000), layer 3 of PFC and temporal cortex (Garey *et al*, 1998), and in the hippocampal formation (Rosoklija *et al*, 2000), although none of these studies have examined auditory cortex. Total dendritic length was found to be reduced in subjects with schizophrenia in the two of these studies that examined this parameter (Glantz and Lewis, 2000; Rosoklija *et al*, 2000), though this change may not be diagnosis specific (Glantz and Lewis, 2000). Thus, both reductions in the extent of dendritic arborization and reduced densities of spines per dendrite may contribute to the reductions in total numbers of dendritic spines in subjects with schizophrenia. Importantly, the convergence of the current findings with the earlier studies using different methods, in different brain regions, suggests that reduced numbers of layer 3 dendritic spines is a conserved abnormality in this disorder.

Effect of Antipsychotic Treatment

SP-IR puncta density did not differ between schizophrenia subjects on or off antipsychotic medications or between monkeys exposed chronically to haloperidol or sham. The effects of antipsychotic exposure on cortical dendritic spine density in Golgi or EM studies have not previously been assessed. Several studies have examined the effect of antipsychotic exposure on spinophilin mRNA or protein expression. Law *et al* (2004a) reported no change in spinophilin mRNA expression in occipitoparietal cortex and hippocampus of rats after 14 days of daily exposure to chlorpromazine 15 mg/kg, haloperidol 1 mg/kg, clozapine 25 mg/kg, olanzapine 5 mg/kg, or risperidone 0.5 mg/kg. Kabbani and Levenson (2006) examined mice exposed for 16 days to daily haloperidol 3 mg/kg or clozapine 4 mg/kg. Haloperidol was associated with a 10.0% decrease, and clozapine with a 12.8% increase, in cortical spinophilin protein expression. Lidow *et al* (2001) similarly examined spinophilin protein expression in multiple cortical regions of rhesus monkeys after 1 year of exposure to haloperidol at a maximal daily dose of 0.35–0.42 mg per kg. They found significantly lower spinophilin protein levels in prefrontal, orbital, cingulate, motor, and entorhinal cortices, but no change in primary visual cortex. Auditory cortex was not tested. As a whole, these studies do not reveal a consistent effect of long-term antipsychotic use that would result in the patterns of increased expression of spinophilin and reduced dendritic spine density that have been observed in studies of subjects with schizophrenia.

Relationship to Death by Suicide

Poor functioning can mediate suicide risk in individuals with schizophrenia (Pompili *et al*, 2007); thus suicide in subjects with schizophrenia might be hypothesized to correlate with more severe underlying brain pathology. However, we did not observe a similar association of death by suicide and reductions in pyramidal cell somal volume or axon terminal density in auditory cortex (Sweet *et al*, 2003, 2004, 2007) or in the PFC (Glantz and Lewis, 1997, 2000; Pierri *et al*, 2001). Alternatively, factors associated with suicide independent of a diagnosis of schizophrenia may be associated with reduced dendritic spine density, though we did not observe a reduction in spine density in PFC in a group of subjects with mood disorders, in whom 73% committed suicide (Glantz and Lewis, 2000).

Correlation with Axon Terminal Density

Dendritic spines are the principal target of excitatory inputs in cerebral cortex (Peters, 2002). The predominant sources of excitatory innervation to dendritic spines in deep layer 3 of BA 41 are projections from intrinsic collaterals that arise from layer-4 and -3 pyramidal cells (Mitani *et al*, 1985; Ojima *et al*, 1991; Wallace *et al*, 1991; Thomson and Bannister, 2003; Linden and Schreiner, 2003). Thalamic projections are also present, but are less extensive (Peters, 2002). The sources of excitatory innervation to deep layer 3 of BA 42 are similar; though this layer also receives feedforward projections from layer 3 of BA 41 (Pandya and Sanides, 1973; Jones *et al*, 1995; Galaburda and Pandya, 1983; Fitzpatrick and Imig, 1980).

In normal developmental processes of synaptogenesis and synaptic refinement, spines and the excitatory terminals that synapse onto them are regulated in tandem (Cohen-Cory, 2002; Hensch, 2005). Similarly, in models of deafferentation, experimentally induced reductions in excitatory inputs can result in reduced dendritic spine density (Cheng *et al*, 1997; Segal *et al*, 2003; McKinney *et al*, 1999). Thus, it is likely that the reduced density of dendritic spines in subjects with schizophrenia is accompanied by a corresponding reduction in density of excitatory axon terminals, resulting in diminished excitatory synaptic connectivity in the affected regions.

This interpretation is supported by evidence that dendritic spine density and density of synaptophysin-immunoreactive axon terminals were correlated within subjects in BA 41 and 42. Several concerns regarding this observation, however, require comment. The magnitude of reductions in dendritic spine density observed in BA 41 and 42, 27.2 and 22.2%, were much greater than the 13.6% reduction in density of synaptophysin-immunoreactive terminals in deep layer 3 of BA 41, and the nonsignificant lowering of density of synaptophysin-immunoreactive terminals by 6.1% in BA 42. These differences may be understood, in part, by noting that synaptophysin is an integral membrane protein of small synaptic vesicles containing classic neurotransmitters, and as a consequence labels approximately 95% of presynaptic terminals in cerebral cortex (Jahn *et al*, 1985; Navone *et al*, 1986), which includes GABAergic inhibitory terminals, monoaminergic terminals, and excitatory terminals that do not synapse onto dendritic spines. Thus, reductions in densities of axospinous excitatory terminals of $\sim$22–27% would result in smaller percent reductions in density of synaptophysin-immunoreactive terminals. Confirmation that excitatory

terminals are reduced in deep layer 3 of BA 41 and 42 in subjects with schizophrenia will require utilizing markers that selectively label excitatory terminals (Kaneko and Fujiyama, 2002).

Lack of Correlation with Pyramidal Cell Somal Volume

Dendritic spine density was not correlated with mean pyramidal cell somal volume in our subjects. The lack of correlation could reflect that spines in deep layer 3 may arise from dendrites of pyramidal cells whose cell bodies are located in other layers. We therefore examined whether basilar dendrite spine density was correlated with cell somal area in the previously reported study of Golgi-impregnated pyramidal cells in deep layer 3 in PFC of subjects with schizophrenia (Glantz and Lewis, 2000). In that study there was a small but significant correlation ($N = 451$ pyramidal cells from 45 subjects, Pearson's $r = 0.117$, $p = 0.01$), suggesting that overall the relationship of pyramidal cell size to dendritic spine density is modest.

Implications for Auditory Cortical Development in Schizophrenia

It has been proposed that reduced excitatory connectivity in subjects with schizophrenia may result either from failure to initially elaborate sufficient numbers of such synapses, excess elimination of these synapses due to experience-dependent plasticity (Grossman *et al*, 2003), or both (Feinberg, 1982; Keshavan *et al*, 1994; Mirnics *et al*, 2001). Our findings cannot differentiate between these three possibilities. However, *in vivo* studies suggest that experience-dependent synaptic elimination in auditory cortex persists into early adulthood (Gogtay *et al*, 2004), and may be accelerated in subjects with schizophrenia (Kasai *et al*, 2003; Salisbury *et al*, 2007). Longitudinal studies of normally developing children using MRI to assess gray matter density have revealed that the time course of reductions in gray matter volume of the STG is protracted relative to other brain regions (other than dorsolateral PFC), continuing into the third decade (Gogtay *et al*, 2004). Similarly, longitudinal studies of subjects with schizophrenia, many of whom were in the third decade of life, have found that auditory cortex gray matter volume loss continues after first hospitalization in a manner that is accelerated relative to control subjects (Kasai *et al*, 2003; Salisbury *et al*, 2007). Progressive reduction of auditory cortex gray matter volume is also correlated with decreasing magnitude of mismatch negativity (MMN), an auditory event-related potential arising from primary auditory cortex (Salisbury *et al*, 2007).

Congruent with *in vivo* observations of normal gray matter volume reductions during adolescence and early adulthood, Rakic *et al* (1986), in a series of studies in nonhuman primate, found that there is a net loss of cortical synapses that occurs most rapidly during adolescence and continues into early adulthood. Synapse elimination was apparent throughout multiple cortical regions, though auditory cortex was not specifically assessed. Excitatory synapses onto dendritic spines, especially within layer 3, undergo the most dramatic elimination during this developmental period (Rakic *et al*, 1986; Bourgeois *et al*, 1994). Thus, a plausible interpretation of the human post-mortem and *in vivo* findings is that pathologic enhancements of those processes that normally result in net elimination of excitatory synapses in layer 3 of auditory cortex contribute to the early disease course in subjects with schizophrenia. This interpretation suggests that interventions at or shortly after the transition to syndromal psychosis may provide for secondary prevention of disease progression.

There has been substantial recent progress in understanding the mechanisms leading to the normal adolescent and early adult experience-dependent refinement of dendritic spines. Even in adult animals, spines are dynamic structures, with continuing generation and retraction of up to 5–20% of spines on cortical pyramidal neurons (Holtmaat *et al*, 2005). Moreover, experience-dependent plasticity modifies existing spine structure, such that long-term potentiation (LTP) results in spine enlargement and stabilization, whereas long-term depression (LTD) can induce spine shrinkage and elimination (Matsuzaki, 2007). The pathways transducing LTP and LTD into structural spine plasticity are similarly beginning to be elucidated (Negishi and Katoh, 2005; Calabrese *et al*, 2006). A compelling hypothesis is that lower dendritic spine density in subjects with schizophrenia results from reduction in factors leading to the generation of new spines and mediating the stabilizing structural effects of LTP, and/or increases in factors mediating the structural effects of LTD.

Some evidence in support of this hypothesis has previously been reported in subjects with schizophrenia. Reduced mRNA expression of cell division cycle 42, which promotes dendritic spine outgrowth (Irie and Yamaguchi, 2002), and Kalirin 7, which is necessary for both spine outgrowth and mediates LTP-induced spine structural plasticity (Penzes *et al*, 2001), was found in PFC, and correlated with reductions in spine density (Hill *et al*, 2006). Of interest, spinophilin has been recently shown to be a mediator of LTD-, but not LTP-induced structural plasticity (Feng *et al*, 2000). These effects are mediated via recruitment of the Rho guanine exchange factor, Lfc (Lbc (lymphoid blast crisis)'s first cousin), into spines (Ryan *et al*, 2005), and via targeting of protein phosphatase 1 to glutamate receptors within spines (Feng *et al*, 2000) and to actin (Fernandez *et al*, 1990). As reviewed above, there is evidence to suggest spinophilin expression is increased or unchanged in cortical extracts of subjects with schizophrenia. However, in the presence of a 20–30% reduction of number of dendritic spines, spinophilin expression per spine may be significantly increased in subjects with schizophrenia, and may enhance LTD-induced spine elimination.

Implications for Auditory Sensory Processing in Schizophrenia

If our findings do reflect a lower number of both the pre- and postsynaptic components of excitatory synaptic connections to pyramidal neurons within deep layer 3 of auditory cortex, several implications for understanding impaired auditory sensory processing in subjects with schizophrenia emerge. Individuals with schizophrenia demonstrate impaired pure tone discrimination (Javitt *et al*, 1997b), with correlated impairments in recognition of auditory emotion (Leitman *et al*, 2005). Subjects with schizophrenia similarly demonstrate reductions in MMN,

which arises in response to auditory stimuli that deviate in one characteristic (eg pitch) from a repetitive stimulus (Javitt *et al*, 2000), and which is likely to tap the same underlying intracortical mechanisms as tone discrimination (Javitt *et al*, 1994).

MMN is assessable in nonhuman primate models, where it has been shown to arise from the spread of activation through the superficial layers of the primary auditory cortex after the initial depolarizing thalamic volley (Javitt *et al*, 1994). This spread is dependent on the intrinsic axon collaterals and their postsynaptic pyramidal cell targets within layer 3 (Figure 1). The reduction in MMN in subjects with schizophrenia appears to represent an inability to generate maximum current flow in these circuits (Javitt *et al*, 1997a) and thus could clearly reflect the reduction we observed in axon terminals and dendritic spines in this layer. Similarly, reductions of MMN analogous to those seen in subjects with schizophrenia can be modeled by the infusion into the auditory cortex of agents that selectively block the *N*-methyl-D-aspartate (NMDA) class of excitatory glutamate receptors (Javitt *et al*, 1994), an observation paralleled by systemic administration of NMDA antagonists in normal humans (Umbricht *et al*, 2000). Because NMDA receptors within pyramidal cells are predominantly located in spines, the observed reduction in spine number may result in a net reduction in NMDA activation and contributes to MMN. However, it remains an open question whether within the remaining spines NMDA signaling is unchanged, up- or downregulated. Methods for quantification of NMDA receptors will need to account for possible confounding by the reduction in spine number itself, and separately account for their presence in spines and at excitatory synapses onto inhibitory neurons (Homayoun and Moghaddam, 2007). Though complex, defining these relationships in subjects with schizophrenia would have substantial impact on refining efforts to effectively develop glutamatergic pharmacotherapies, an approach that to date has met with some, albeit limited, success (Tuominen *et al*, 2006).

ACKNOWLEDGEMENTS

This work was supported by USPHS grants MH 045156 and MH 071533 and by the VISN 4 Mental Illness Research, Education and Clinical Center, VA Pittsburgh Healthcare System. The content is solely the responsibility of the authors and does not necessarily represent the official views of the National Institute of Mental Health or the National Institutes of Health. We thank Dr Ken Fish for the conduct of the primary neuronal culture assessment of antibody specificity, and Mrs Mary Brady for assistance with the figures. We acknowledge the efforts of the research staff of the Translational Neuroscience Program and the Conte Center for Neuroscience of Mental Disorders at the University of Pittsburgh.

DISCLOSURE/CONFLICT OF INTEREST

Dr David A Lewis currently receives research support from the BMS Foundation, Merck and Pfizer and in 2006–2008 served as a consultant to Bristol-Meyer Squibb, Lilly, Merck, Neurogen, Pfizer, Hoffman-Roche, Sepracor, and Wyeth. Allan R Sampson serves as consultant to Johnson & Johnson Pharmaceutical Research and Development and Winston Laboratories, and in 2006–2007 served as a consultant to Bristol-Meyer Squibb and Pain Therapeutics. Robert A Sweet, Ruth A Henteleff, and Wei Zhang have no conflicts of interest to disclose.

REFERENCES

Akil M, Pierri JN, Whitehead RE, Edgar CL, Mohila C, Sampson AR *et al* (1999). Lamina-specific alterations in the dopamine innervation of the prefrontal cortex in schizophrenic subjects. *Am J Psychiatry* **156**: 1580–1589.

Akram A, Christoffel D, Rocher AB, Bouras C, Kövari E, Perl DP *et al* (2007). Stereologic estimates of total spinophilin-immunoreactive spine number in area 9 and the CA1 field: relationship with the progression of Alzheimer's disease. *Neurobiol Aging*; e-pub ahead of print 7 April 2007.

Allen PB, Ouimet CC, Greengard P (1997). Spinophilin, a novel protein phosphatase 1 binding protein localized to dendritic spines. *Proc Natl Acad Sci USA* **94**: 9956–9961.

Amateau SK, McCarthy MM (2002). A novel mechanism of dendritic spine plasticity involving estradiol induction of prostaglandin-E2. *J Neurosci* **22**: 8586–8596.

American Psychiatric Association (1987). *Diagnostic and Statistical Manual of Mental Disorders*, 3rd edn, Revised. American Psychiatric Association: Washington, DC.

Aridor M, Guzik AK, Bielli A, Fish KN (2004). Endoplasmic reticulum export site formation and function in dendrites. *J Neurosci* **24**: 3770–3776.

Baracskay KL, Haroutunian V, Meador-Woodruff JH (2006). Dopamine receptor signaling molecules are altered in elderly schizophrenic cortex. *Synapse* **60**: 271–279.

Barta PE, Pearlson GD, Brill II LB, Royall R, McGilchrist IK, Pulver AE *et al* (1997). Planum temporale asymmetry reversal in schizophrenia: replication and relationship to gray matter abnormalities. *Am J Psychiatry* **154**: 661–667.

Bourgeois JP, Goldman-Rakic PS, Rakic P (1994). Synaptogenesis in the prefrontal cortex of rhesus monkeys. *Cereb Cortex* **4**: 78–96.

Braendgaard H, Evans SM, Howard CV, Gundersen HJ (1990). The total number of neurons in the human neocortex unbiasedly estimated using optical disectors. *J Microsc* **157** (Part 3): 285–304.

Calabrese B, Wilson MS, Halpain S (2006). Development and regulation of dendritic spine synapses. *Physiology (Bethesda)* **21**: 38–47.

Capani F, Deerinck TJ, Ellisman MH, Bushong E, Bobik M, Martone ME (2001). Phalloidin-eosin followed by photo-oxidation: a novel method for localizing F-actin at the light and electron microscopic levels. *J Histochem Cytochem* **49**: 1351–1361.

Cheng HW, Rafols JA, Goshgarian HG, Anavi Y, Tong J, McNeill TH (1997). Differential spine loss and regrowth of striatal neurons following multiple forms of deafferentation: a Golgi study. *Exp Neurol* **147**: 287–298.

Clinton SM, Ibrahim HM, Frey KA, Davis KL, Haroutunian V, Meador-Woodruff JH (2005). Dopaminergic abnormalities in select thalamic nuclei in schizophrenia: involvement of the intracellular signal integrating proteins calcyon and spinophilin. *Am J Psychiatry* **162**: 1859–1871.

Cohen-Cory S (2002). The developing synapse: construction and modulation of synaptic structures and circuits. *Science* **298**: 770–776.

Dorph-Petersen KA, Nyengaard JR, Gundersen HJ (2001). Tissue shrinkage and unbiased stereological estimation of particle number and size. *J Microsc* **204**: 232–246.

Falkai P, Bogerts B, Schneider T, Greve B, Pfeiffer U, Pilz K *et al* (1995). Disturbed planum temporale asymmetry in schizophrenia. A quantitative post-mortem study. *Schizophr Res* **14**: 161–176.

Feinberg I (1982). Schizophrenia: caused by a fault in programmed synaptic elimination during adolescence? *J Psychiatr Res* **17**: 319–334.

Feng J, Yan Z, Ferreira A, Tomizawa K, Liauw JA, Zhuo M *et al* (2000). Spinophilin regulates the formation and function of dendritic spines. *Proc Natl Acad Sci USA* **97**: 9287–9292.

Fernandez A, Brautigan DL, Mumby M, Lamb NJ (1990). Protein phosphatase type-1, not type-2A, modulates actin microfilament integrity and myosin light chain phosphorylation in living nonmuscle cells. *J Cell Biol* **111**: 103–112.

Fitzpatrick K, Imig J (1980). Auditory cortico-cortical connections in the owl monkey. *J Comp Neurol* **192**: 589–610.

Galaburda AM, Pandya DN (1983). The intrinsic architectonic and connectional organization of the superior temporal region of the rhesus monkey. *J Comp Neurol* **221**: 169–184.

Garey LJ, Ong WY, Patel TS, Kanani M, Davis A, Mortimer AM *et al* (1998). Reduced dendritic spine density on cerebral cortical pyramidal neurons in schizophrenia. *J Neurol Neurosurg Psychiatry* **65**: 446–453.

Glantz LA, Lewis DA (1997). Reduction of synaptophysin immunoreactivity in the prefrontal cortex of subjects with schizophrenia. Regional and diagnostic specificity (corrected and republished article originally appeared in *Arch Gen Psychiatry* 1997 54:660–669). *Arch Gen Psychiatry* **54**: 943–952.

Glantz LA, Lewis DA (2000). Decreased dendritic spine density on prefrontal cortical pyramidal neurons in schizophrenia. *Arch Gen Psychiatry* **57**: 65–73.

Gogtay N, Giedd JN, Lusk L, Hayashi KM, Greenstein D, Vaituzis AC *et al* (2004). Dynamic mapping of human cortical development during childhood through early adulthood. *Proc Natl Acad Sci USA* **101**: 8174–8179.

Goldstein JM, Goodman JM, Seidman LJ, Kennedy DN, Makris N, Lee H *et al* (1999). Cortical abnormalities in schizophrenia identified by structural magnetic resonance imaging. *Arch Gen Psychiatry* **56**: 537–547.

Grossman AW, Churchill JD, McKinney BC, Kodish IM, Otte SL, Greenough WT (2003). Experience effects on brain development: possible contributions to psychopathology. *J Child Psychol Psychiatry* **44**: 33–63.

Gundersen HJ (1986). Stereology of arbitrary particles. A review of unbiased number and size estimators and the presentation of some new ones, in memory of William R. Thompson. *J Microsc* **143**(Part 1): 3–45.

Gundersen HJ, Jensen EB, Kieu K, Nielsen J (1999). The efficiency of systematic sampling in stereology—reconsidered. *J Microsc* **193**: 199–211.

Hao J, Janssen WG, Tang Y, Roberts JA, McKay H, Lasley B *et al* (2003). Estrogen increases the number of spinophilin-immunoreactive spines in the hippocampus of young and aged female rhesus monkeys. *J Comp Neurol* **465**: 540–550.

Hashikawa T, Molinari M, Rausell E, Jones EG (1995). Patchy and laminar terminations of medial geniculate axons in monkey auditory cortex. *J Comp Neurol* **362**: 195–208.

Hensch TK (2005). Critical period plasticity in local cortical circuits. *Nat Rev Neurosci* **6**: 877–888.

Highley JR, McDonald B, Walker MA, Esiri MM, Crow TJ (1999). Schizophrenia and temporal lobe asymmetry: a post-mortem stereological study of tissue volume. *Br J Psychiatry* **175**: 127–134.

Hill JJ, Hashimoto T, Lewis DA (2006). Molecular mechanisms contributing to dendritic spine alterations in the prefrontal cortex of subjects with schizophrenia. *Mol Psychiatry* **11**: 557–566.

Hirayasu Y, McCarley RW, Salisbury DF, Tanaka S, Kwon JS, Frumin M *et al* (2000). Planum temporale and Heschl gyrus volume reduction in schizophrenia: a magnetic resonance imaging study of first-episode patients. *Arch Gen Psychiatry* **57**: 692–699.

Hirayasu Y, Shenton ME, Salisbury DF, Dickey CC, Fischer IA, Mazzoni P *et al* (1998). Lower left temporal lobe MRI volumes in patients with first-episode schizophrenia compared with psychotic patients with first-episode affective disorder and normal subjects. *Am J Psychiatry* **155**: 1384–1391.

Holtmaat AJ, Trachtenberg JT, Wilbrecht L, Shepherd GM, Zhang X, Knott GW *et al* (2005). Transient and persistent dendritic spines in the neocortex *in vivo*. *Neuron* **45**: 279–291.

Homayoun H, Moghaddam B (2007). NMDA receptor hypofunction produces opposite effects on prefrontal cortex interneurons and pyramidal neurons. *J Neurosci* **27**: 11496–11500.

Honea R, Crow TJ, Passingham D, Mackay CE (2005). Regional deficits in brain volume in schizophrenia: a meta-analysis of voxel-based morphometry studies. *Am J Psychiatry* **162**: 2233–2245.

Ingham CA, Hood SH, van Maldegem B, Weenink A, Arbuthnott GW (1993). Morphological changes in the rat neostriatum after unilateral 6-hydroxydopamine injections into the nigrostriatal pathway. *Exp Brain Res* **93**: 17–27.

Irie F, Yamaguchi Y (2002). EphB receptors regulate dendritic spine development via intersectin, Cdc42 and N-WASP. *Nat Neurosci* **5**: 1117–1118.

Jahn R, Schiebler W, Ouimet C, Greengard P (1985). A 38 000-dalton membrane protein (p38) present in synaptic vesicles. *Proc Natl Acad Sci USA* **82**: 4137–4141.

Javitt DC, Doneshka P, Grochowski S, Ritter W (1995). Impaired mismatch negativity generation reflects widespread dysfunction of working memory in schizophrenia. *Arch Gen Psychiatry* **52**: 550–558.

Javitt DC, Grochowski S, Shelley AM, Ritter W (1997a). Impaired mismatch negativity (MMN) generation in schizophrenia as a function of stimulus deviance, probability, and interstimulus/interdeviant interval. *Electroencephalogr Clin Neurophysiol* **108**: 143–153.

Javitt DC, Shelley AM, Ritter W (2000). Associated deficits in mismatch negativity generation and tone matching in schizophrenia. *Clin Neurophysiol* **111**: 1733–1737.

Javitt DC, Steinschneider M, Schroeder CE, Vaughan HG, Arezzo JC (1994). Detection of stimulus deviance within primate primary auditory cortex: intracortical mechanisms of mismatch negativity (MMN) generation. *Brain Res* **667**: 192–200.

Javitt DC, Strous RD, Grochowski S, Ritter W, Cowan N (1997b). Impaired precision, but normal retention, of auditory sensory ('echoic') memory information in schizophrenia. *J Abnorm Psychol* **106**: 315–324.

Jones EG, Dell'Anna ME, Molinari M, Rausell E, Hashikawa T (1995). Subdivisions of macaque monkey auditory cortex revealed by calcium-binding protein immunoreactivity. *J Comp Neurol* **362**: 153–170.

Kabbani N, Levenson R (2006). Antipsychotic-induced alterations in D2 dopamine receptor interacting proteins within the cortex. *Neuroreport* **17**: 299–301.

Kaneko T, Fujiyama F (2002). Complementary distribution of vesicular glutamate transporters in the central nervous system. *Neurosci Res* **42**: 243–250.

Kasai K, Shenton ME, Salisbury DF, Hirayasu Y, Onitsuka T, Spencer MH *et al* (2003). Progressive decrease of left Heschl gyrus and planum temporale gray matter volume in first-episode schizophrenia: a longitudinal magnetic resonance imaging study. *Arch Gen Psychiatry* **60**: 766–775.

Keshavan MS, Anderson S, Pettegrew JW (1994). Is schizophrenia due to excessive synaptic pruning in the prefrontal cortex? The Feinberg hypothesis revisited. *J Psychiatr Res* **28**: 239–265.

Koh PO, Bergson C, Undie AS, Goldman-Rakic PS, Lidow MS (2003). Up-regulation of the D1 dopamine receptor-interacting

protein, calcyon, in patients with schizophrenia. *Arch Gen Psychiatry* **60**: 311–319.

Konopaske GT, Dorph-Petersen KA, Sweet RA, Pierri JN, Zhang W, Sampson AR *et al* (2008). Effect of chronic antipsychotic exposure on astrocyte and oligodendrocyte numbers in macaque monkeys. *Biol Psychiatry* **63**: 759–765.

Kwon JS, McCarley RW, Hirayasu Y, Anderson JE, Fischer IA, Kikinis R *et al* (1999). Left planum temporale volume reduction in schizophrenia. *Arch Gen Psychiatry* **56**: 142–148.

Law AJ, Hutchinson LJ, Burnet PW, Harrison PJ (2004a). Antipsychotics increase microtubule-associated protein 2 mRNA but not spinophilin mRNA in rat hippocampus and cortex. *J Neurosci Res* **76**: 376–382.

Law AJ, Weickert CS, Hyde TM, Kleinman JE, Harrison PJ (2004b). Reduced spinophilin but not microtubule-associated protein 2 expression in the hippocampal formation in schizophrenia and mood disorders: molecular evidence for a pathology of dendritic spines. *Am J Psychiatry* **161**: 1848–1855.

Lee CC, Imaizumi K, Schreiner CE, Winer JA (2004). Concurrent tonotopic processing streams in auditory cortex. *Cereb Cortex* **14**: 441–451.

Leitman DI, Foxe JJ, Butler PD, Saperstein A, Revheim N, Javitt DC (2005). Sensory contributions to impaired prosodic processing in schizophrenia. *Biol Psychiatry* **58**: 56–61.

Leranth C, Shanabrough M, Redmond Jr DE (2002). Gonadal hormones are responsible for maintaining the integrity of spine synapses in the CA1 hippocampal subfield of female nonhuman primates. *J Comp Neurol* **447**: 34–42.

Lewis DA, Cruz DA, Melchitzky DS, Pierri JN (2001). Lamina-specific deficits in parvalbumin-immunoreactive varicosities in the prefrontal cortex of subjects with schizophrenia: evidence for fewer projections from the thalamus. *Am J Psychiatry* **158**: 1411–1422.

Lidow MS, Song ZM, Castner SA, Allen PB, Greeengard P, Goldman-Rakic PS (2001). Antipsychotic treatment induces alterations in dendrite-and-spine associated proteins in dopamine rich areas of the primate cerebral cortex. *Biol Psychiatry* **49**: 1–12.

Liegeois-Chauvel C, Lorenzi C, Trebuchon A, Regis J, Chauvel P (2004). Temporal envelope processing in the human left and right auditory cortices. *Cereb Cortex* **14**: 731–740.

Linden JF, Schreiner CE (2003). Columnar transformations in auditory cortex? A comparison to visual and somatosensory cortices. *Cereb Cortex* **13**: 83–89.

Littell RC, Milliken GA, Stroup WW, Wolfinger RD (1996). *SAS System for Mixed Models*. SAS Institute Inc.: Cary, NC.

Marcsisin MJ, Dorph-Petersen KA, Gundersen HJG, Sampson AR, Lewis DA, Sweet RA (2007). Gray matter volume is selectively reduced in supragranular layers of the auditory parabelt cortex in subjects with schizophrenia (abstract). *Biol Psychiatry* **61**: 159–160.

Mathalon DH, Pfefferbaum A, Lim KO, Rosenblum MA, Sullivan EV (2003). Compounded brain volume deficits in schizophrenia-alcoholism comorbidity. *Arch Gen Psychiatry* **60**: 245–252.

Mathalon DH, Sullivan EV, Lim KO, Pfefferbaum A (2001). Progressive brain volume changes and the clinical course of schizophrenia in men. *Arch Gen Psychiatry* **58**: 148–157.

Matsuzaki M (2007). Factors critical for the plasticity of dendritic spines and memory storage. *Neurosci Res* **57**: 1–9.

McCarley RW, Faux SF, Shenton ME, Nestor PG, Adams J (1991). Event-related potentials in schizophrenia: their biological and clinical correlates and a new model of schizophrenic pathophysiology. *Schizophr Res* **4**: 209–231.

McCarley RW, Wible CG, Frumin M, Hirayasu Y, Levitt JJ, Fischer IA *et al* (1999). MRI anatomy of schizophrenia. *Biol Psychiatry* **45**: 1099–1119.

McKinney RA, Capogna M, Durr R, Gahwiler BH, Thompson SM (1999). Miniature synaptic events maintain dendritic spines via AMPA receptor activation. *Nat Neurosci* **2**: 44–49.

Mirnics K, Middleton FA, Lewis DA, Levitt P (2001). Analysis of complex brain disorders with gene expression microarrays: schizophrenia as a disease of the synapse. *Trends Neurosci* **24**: 479–486.

Mitani A, Shimokouchi M, Itoh K, Nomura S, Kudo M, Mizuno N (1985). Morphology and laminar organization of electrophysiologically identified neurons in the primary auditory cortex in the cat. *J Comp Neurol* **235**: 430–447.

Molinari M, Dell'Anna ME, Rausell E, Leggio MG, Hashikawa T, Jones EG (1995). Auditory thalamocortical pathways defined in monkeys by calcium-binding protein immunoreactivity. *J Comp Neurol* **362**: 171–194.

Muly EC, Smith Y, Allen P, Greengard P (2004). Subcellular distribution of spinophilin immunolabeling in primate prefrontal cortex: localization to and within dendritic spines. *J Comp Neurol* **469**: 185–197.

Navone F, Jahn R, Di Gioia G, Stukenbrok H, Greengard P, De Camilli P (1986). Protein p38: an integral membrane protein specific for small vesicles of neurons and neuroendocrine cells. *J Cell Biol* **103**: 2511–2527.

Negishi M, Katoh H (2005). Rho family GTPases and dendrite plasticity. *Neuroscientist* **11**: 187–191.

Ojima H, Honda CN, Jones EG (1991). Patterns of axon collateralization of identified supragranular pyramidal neurons in the cat auditory cortex. *Cereb Cortex* **1**: 80–94.

Pandya DN, Rosene DL (1993). Laminar termination patterns of thalamic, callosal, and association afferents in the primary auditory area of the rhesus monkey. *Exp Neurol* **119**: 220–234.

Pandya DN, Rosene DL, Doolittle AM (1994). Corticothalamic connections of auditory-related areas of the temporal lobe in the rhesus monkey. *J Comp Neurol* **345**: 447–471.

Pandya DN, Sanides F (1973). Architectonic parcellation of the temporal operculum in rhesus monkey and its projection pattern. *Z Anat Entwickl-Gesch* **139**: 127–161.

Penzes P, Johnson RC, Sattler R, Zhang X, Huganir RL, Kambampati V *et al* (2001). The neuronal Rho-GEF Kalirin-7 interacts with PDZ domain-containing proteins and regulates dendritic morphogenesis. *Neuron* **29**: 229–242.

Peters A (2002). Examining neocortical circuits: some background and facts. *J Neurocytol* **31**: 183–193.

Pierri JN, Volk CL, Auh S, Sampson A, Lewis DA (2001). Decreased somal size of deep layer 3 pyramidal neurons in the prefrontal cortex of subjects with schizophrenia. *Arch Gen Psychiatry* **58**: 466–473.

Pompili M, Amador XF, Girardi P, Harkavy-Friedman J, Harrow M, Kaplan K *et al* (2007). Suicide risk in schizophrenia: learning from the past to change the future. *Ann Gen Psychiatry* **6**: 10.

Rabinowicz EF, Silipo G, Goldman R, Javitt DC (2000). Auditory sensory dysfunction in schizophrenia: imprecision or distractibility? *Arch Gen Psychiatry* **57**: 1149–1155.

Rajarethinam R, Sahni S, Rosenberg DR, Keshavan MS (2004). Reduced superior temporal gyrus volume in young offspring of patients with schizophrenia. *Am J Psychiatry* **161**: 1121–1124.

Rajkowska G, Selemon LD, Goldman-Rakic PS (1998). Neuronal and glial somal size in the prefrontal cortex: a postmortem morphometric study of schizophrenia and Huntington disease. *Arch Gen Psychiatry* **55**: 215–224.

Rakic P, Bourgeois JP, Eckenhoff MF, Zecevic N, Goldman-Rakic PS (1986). Concurrent overproduction of synapses in diverse regions of the primate cerebral cortex. *Science* **232**: 232–235.

Rosoklija G, Toomayan G, Ellis SP, Keilp J, Mann JJ, Latov N *et al* (2000). Structural abnormalities of subicular dendrites in subjects with schizophrenia and mood disorders. *Arch Gen Psychiatry* **57**: 349–356.

Ryan XP, Alldritt J, Svenningsson P, Allen PB, Wu GY, Nairn AC *et al* (2005). The Rho-specific GEF Lfc interacts with neurabin and spinophilin to regulate dendritic spine morphology. *Neuron* **47**: 85–100.

Salisbury DF, Kuroki N, Kasai K, Shenton ME, McCarley RW (2007). Progressive and interrelated functional and structural evidence of post-onset brain reduction in schizophrenia. *Arch Gen Psychiatry* **64**: 521–529.

Sanfilpo M, Lafargue T, Rusinek H, Arena L, Loneragan C, Lautin A *et al* (2000). Volumetric measure of the frontal and temporal lobe regions in schizophrenia. *Arch Gen Psychiatry* **57**: 471–480.

Scheff SW, Price DA (2003). Synaptic pathology in Alzheimer's disease: a review of ultrastructural studies. *Neurobiol Aging* **24**: 1029–1046.

Segal M, Greenberger V, Korkotian E (2003). Formation of dendritic spines in cultured striatal neurons depends on excitatory afferent activity. *Eur J Neurosci* **17**: 2573–2585.

Shenton ME, Kikinis R, Jolesz FA, Pollak SD, LeMay M, Wible CG *et al* (1992). Abnormalities of the left temporal lobe and thought disorder in schizophrenia. A quantitative magnetic resonance imaging study. *N Engl J Med* **327**: 612.

Shergill SS, Brammer MJ, Williams SCR, Murray RM, McGuire PK (2000). Mapping auditory hallucinations in schizophrenia using functional magnetic resonance imaging. *Arch Gen Psychiatry* **57**: 1033–1038.

Sigmundsson T, Suckling J, Williams SCR, Bullmore ET, Greenwood KE, Fukuda R *et al* (2001). Structural abnormalities in frontal, temporal and limbic regions and interconnecting white matter tracts in schizophrenic patients with prominent negative symptoms. *Am J Psychiatry* **158**: 234–243.

Strous RD, Cowan N, Ritter W, Javitt DC (1995). Auditory sensory ('echoic') memory dysfunction in schizophrenia. *Am J Psychiatry* **152**: 1517–1519.

Sullivan EV, Mathalon DH, Lim KO, Marsh L, Pfefferbaum A (1998). Patterns of regional cortical dysmorphology distinguishing schizophrenia and chronic alcoholism. *Biol Psychiatry* **43**: 118–131.

Sweet RA, Bergen SE, Sun Z, Marcsisin MJ, Sampson AR, Lewis DA (2007). Anatomical evidence of impaired feedforward auditory processing in schizophrenia. *Biol Psychiatry* **61**: 854–864.

Sweet RA, Bergen SE, Sun Z, Sampson AR, Pierri JN, Lewis DA (2004). Pyramidal cell size reduction in schizophrenia: evidence for involvement of auditory feedforward circuits. *Biol Psychiatry* **55**: 1128–1137.

Sweet RA, Dorph-Petersen KA, Lewis DA (2005). Mapping auditory core, lateral belt, and parabelt cortices in the human superior temporal gyrus. *J Comp Neurol* **491**: 270–289.

Sweet RA, Pierri JN, Auh S, Sampson AR, Lewis DA (2003). Reduced pyramidal cell somal volume in auditory association cortex of subjects with schizophrenia. *Neuropsychopharmacology* **28**: 599–609.

Tang Y, Janssen WG, Hao J, Roberts JA, McKay H, Lasley B *et al* (2004). Estrogen replacement increases spinophilin-immunoreactive spine number in the prefrontal cortex of female rhesus monkeys. *Cereb Cortex* **14**: 215–223.

Thomson AM, Bannister AP (2003). Interlaminar connections in the neocortex. *Cereb Cortex* **13**: 5–14.

Tuominen HJ, Tiihonen J, Wahlbeck K (2006). Glutamatergic drugs for schizophrenia. *Cochrane Database Syst Rev* 19 April 2006; (2): CD003730.

Umbricht D, Schmid L, Koller R, Vollenweider FX, Hell D, Javitt DC (2000). Ketamine-induced deficits in auditory and visual context-dependent processing in healthy volunteers: implications for models of cognitive deficits in schizophrenia. *Arch Gen Psychiatry* **57**: 1139–1147.

Vogeley K, Hobson T, Schneider-Axmann T, Honer WG, Bogerts B, Falkai P (1998). Compartmental volumetry of the superior temporal gyrus reveals sex differences in schizophrenia-a post-mortem study. *Schizophr Res* **31**: 83–87.

Volavka J, Cooper T, Czobor P, Bitter I, Meisner M, Laska E *et al* (1992). Haloperidol blood levels and clinical effects. *Arch Gen Psychiatry* **49**: 354–361.

Wallace MN, Kitzes LM, Jones EG (1991). Intrinsic inter- and intralaminar connections and their relationship to the tonotopic map in cat primary auditory cortex. *Exp Brain Res* **86**: 527–544.

Watts J, Thomson AM (2005). Excitatory and inhibitory connections show selectivity in the neocortex. *J Physiol* **562**: 89–97.

Weickert CS, Straub RE, McClintock BW, Matsumoto M, Hashimoto R, Hyde TM *et al* (2004). Human dysbindin (DTNBP1) gene expression in normal brain and in schizophrenic prefrontal cortex and midbrain. *Arch Gen Psychiatry* **61**: 544–555.

Wessinger CM, VanMeter J, Tian B, Van Lare J, Pekar J, Rauschecker JP (2001). Hierarchical organization of the human auditory cortex revealed by functional magnetic resonance imaging. *J Cogn Neurosci* **13**: 1–7.

Wexler BE, Stevens AA, Bowers AA, Sernyak MJ, Goldman-Rakic PS (1998). Word and tone working memory deficits in schizophrenia. *Arch Gen Psychiatry* **55**: 1093–1096.

Supplementary Information accompanies the paper on the *Neuropsychopharmacology* website (http://www.nature.com/npp)